Journal of Hazardous Materials 186 (2011) 1124–1130

Contents lists available at ScienceDirect

Journal of Hazardous Materials

journal homepage: www.elsevier.com/locate/jhazmat

Photocatalytic reduction of Cr(VI) on the new hetero-system $CuAl_2O_4/TiO_2$

R. Gherbi [a], N. Nasrallah [a,b], A. Amrane [b], R. Maachi [a], M. Trari [c,*]

[a] Laboratory of Reaction Engineering, Faculty of Mechanic and Engineering Processes, USTHB, BP 32, 16111 Algiers, Algeria
[b] Equipe chimie et Ingénierie des procédés, UMR CNRS 6226, E.N.S.C.R., Avenue du Général Leclerc, CS 50837, 35708 Rennes Cedex 7, France
[c] Laboratory of Storage and Valorization of Renewable Energies, Faculty of Chemistry, USTHB, BP 32, 16111 Algiers, Algeria

ARTICLE INFO

Article history:
Received 3 August 2010
Received in revised form 1 November 2010
Accepted 26 November 2010
Available online 3 December 2010

Keywords:
Photocatalytic
$CuAl_2O_4$
Cr(VI)
Salicylic acid
TiO_2
Hydrogen

ABSTRACT

Visible light driven $HCrO_4^-$ reduction was successfully achieved over the new hetero-system $CuAl_2O_4/TiO_2$. The spinel, elaborated by nitrate route, was characterized photo electrochemically. The optical gap was found to be 1.70 eV and the transition is directly allowed. The conduction band ($-1.05\ V_{SCE}$) is located below that of TiO_2, more negative than the $HCrO_4^-/Cr^{3+}$ level ($+0.58\ V_{SCE}$) yielding a thermodynamically feasible chromate reduction upon visible illumination. $CuAl_2O_4$ is stable against photo corrosion by holes consumption reaction involving salicylic acid which favors the charges separation. There is a direct correlation between the dark adsorption and the photo activity. A reduction of more than 95% of chromate was achieved after 3 h irradiation at pH 2 with an optimal mass ratio ($CuAl_2O_4/TiO_2$) equal to 1/3. The reduction follows a first order kinetic with a half life of ~1 h and a quantum yield of 0.11% under polychromatic light. Prolonged illumination was accompanied by a deceleration of the Cr(VI) reduction thanks to the competitive water discharge. The hydrogen evolution, an issue of energetic concern, took place with a rate of 3.75 cm^3 (g catalyst)$^{-1}$ h^{-1}.

1. Introduction

Chromium is extensively used in various industrial applications like electroplating, leather tanning, refractory industry and metallurgy [1,2]. It occurs mainly in two oxidation states namely VI and III and is released in the aquatic environment at the hexavalent state either as $Cr_2O_7^{2-}$ or $HCrO_4^-$ depending on the pH ($Cr_2O_7^{2-} + H_2O \rightarrow 2HCrO_4^-$, $pK_a = 1.68$). It is now well established that Cr(VI) is one of the major pollutants in wastewater; it is highly toxic and its solubility contributes to the environmental pollution. The World Health Organization maximum level in water is restricted to 5 mg L^{-1}. Therefore, its removal has been actively investigated by many techniques such as cross flow microfiltration [3], reverse osmosis [4] and ion exchange [5]. Such methods are expensive and often inefficient at low concentrations. So, it turns out that the prospect of developing more efficient and durable systems becomes necessary. The photocatalysis has proved its usefulness in the water treatment [6] and requires mild operating conditions. It is based on the illumination of a semiconductor (SC) with energetic photons which generate electron–hole (e^-/h^+) pairs resulting in photo redox processes where Cr(VI) is reduced to less harmful oxidation state namely Cr(III) [7]. The latter is readily precipitated as hydroxide or adsorbed on a variety of substrates. On the other hand, many optically active compounds have been used to reduce inorganic ions [8]. Some researchers studied the Cr(VI) photoreduction on TiO_2 related compounds in presence of organic acids [9–13] and reported the synergistic effect with the oxidation of acids. The studies were extended to other catalysts like $BiVO_4$ [14] and ZnO [15]. Most photoelectrochemical (PEC) studies focused on oxides because of their long term chemical stability. They are important in the environmental remediation, particularly for the elimination of heavy metals which are non biodegradable unlike organic pollutants [16]. However, their forbidden bands are far too large to make efficient the sun spectrum. In addition, the band edges do not span the redox levels in solution and hamper considerably their utilization. Two contradictory factors may be thought of as governing the efficiency, the flat band potential (V_{fb}) and the band gap (E_g). This results from the deep lying valence band (VB) made up of O^{2-}: *2p* orbital (~7 eV below vacuum) whereas the conduction band (CB) derives generally from cationic character [17]. On the other hand, the serious handicap of non-oxide SCs is their susceptibility to photo driven corrosion. A chemical stability and cathodic flat band potential for *p* type specimen are generally counterbalanced by a large gap. This drawback can be overcome by introduction of cationic orbital VB which raises the energy and reduces the gap. In this regard, the spinels have attracted much attention as photocatalysts due to their ability to reduce water under visible illumination [18]. Among the congeners, $CuAl_2O_4$ has interesting photocatalytic properties [19]. In addition, it is stable over a wide pH range, low cost and non-toxic.

* Corresponding author. Tel.: +213 21 24 79 60; fax: +213 21 24 80 08.
E-mail address: solarchemistry@gmail.com (M. Trari).

0304-3894/$ – see front matter © 2010 Elsevier B.V. All rights reserved.
doi:10.1016/j.jhazmat.2010.11.105

The photo reactions are often carried out in dispersion of submicron material in highly divided form [20] and a good catalytic activity is related to a large specific surface area which favors the ions adsorption. However, the spinels suffer from a high rate of bulk recombination, originating from narrow bands. One strategy is to reduce the crystallite size below the minority-carriers diffusion length; hence the electrons have high probability of diffusing into the electric-field region, i.e. the depletion width. So, $CuAl_2O_4$ elaborated by nitrate route increases the amount of reaction per mass ratio and decreases the crystallite size. This approach is flawed since it does not permit large mobility for both carriers (electrons and holes). A performent *p* type photo cathode requires a narrow gap (E_g) and a matching of redox potential close to CB thus improving the stability. However, the photoelectrons on $CuAl_2O_4$-CB cannot be easily captured by $HCrO_4^-$ ions because of the large potential difference which, in acidic media, exceeds 1 V giving rise to a weak activity.

On the other hand, TiO_2 has been actively used in photocatalysis but has light passing over the whole visible spectrum [21]. Some alternatives have been attempted to improve its activity by shifting the spectral photo response toward longer wavelengths. A straightforward solution would be the utilization of heterojunctions where little systematic work has been done because of the difficulty of adjusting suitably the electronic bands of SCs. According to us, there are no papers dealing with clean route for the photocatalytic Cr(VI) on hetero system. An improvement has been reported recently with $CuAlO_2/TiO_2$ by some of us [22]. We report here the $HCrO_4^-$ reduction over the hetero-system $CuAl_2O_4/TiO_2$. Both compounds exhibit an excellent chemical stability and have been used separately as stable photo catalysts. $CuAl_2O_4$ excited with visible light acts as electrons pump resulting from their injection into TiO_2-CB which in turn causes the Cr(VI) reduction. Simultaneously, the hydrogen production which is not negligible was investigated under the same working conditions. Indeed, the search of alternative energy supplies becomes a problem of high priority. Hydrogen is a clean energy carrier which contributes to the environmental protection by reducing the greenhouse gas emission. It meets a growing demand and is attractive for large scale production from the solar energy.

2. Experimental procedures

$CuAl_2O_4$ was prepared by co-precipitation. CuO (prefired at 400 °C) and $Al(NO_3)_2\ 9H_2O$, both of purity greater than 99.5%, were dissolved in HNO_3 (6 N) and the solution was dehydrated in a sand bath until dryness. Then, the powder was denitrified over flame and fired in open alumina crucible standing in a vertical oven at 900 °C. TiO_2 has been the object of nano-sized effect inquiry. It was synthesized by sol gel according to the method described elsewhere [23] which is advantageous for obtaining porous material with large active surface. The technique consists of dissolving $Ti(OC_3H_7)_4$ in methanol/ethanol solution in a molar ratio (1/1/10). The solution was heated at 75 °C for 3 h after which water was added dropwise. The gel was dried overnight and heated at 450° (2 h, 3 °C min^{-1}). Powder X-ray diffraction using Cu Kα radiation (λ = 0.154178 nm) was used to identify the crystalline phases. The electrical contact was established by soldering silver paint on the back pellet with copper wire, the pellets were encapsulated in glass holders using epoxy resin. The electrochemical characterization was done in a three-compartment cell. The exposed area (*A*) of the working electrode was 0.2 cm^2 and Pt sheet (1 cm^2) served as auxiliary electrode. The potentials were monitored by a PGZ301 potentiostat (Radiometer analytical) and measured against a saturated calomel electrode (SCE) by appropriate positioning of the lugging capillary in order to have negligible potential drop. The chrono-potentiometric profile was performed in the working solution $CuAl_2O_4/TiO_2/HCrO_4^-$ using Pt as indicator electrode. The photocurrent–photovoltage (J_{ph}–U_{ph}) curves were recorded in two electrode cell with external resistance boxes and two multimeters (Tacussel, ARIES 2000).

The photocatalytic tests were carried out in a double walled Pyrex reactor of 600 cm^3 capacity whose temperature was regulated at 30 ± 1 °C by a thermostated bath (Julabo). The solutions were deliberately polluted by $K_2Cr_2O_7$ (Merck, purity > 99.5%); the initial concentration was set at 30 ppm and the pH was adjusted at 2 with H_2SO_4. The solubility of salicylic acid is poor in water and the concentration was maintained at 5×10^{-4} M. The air equilibrated dispersion was magnetically stirred under constant agitation. The light source was 200 W tungsten lamp disposed at 10 cm above the reactor in order to maintain a constant light flux (11.4 mW/cm^2). The light was turned on after a transition period (2 h) for the dark adsorption, and the aliquots (5 cm^3) were taken at periodic time intervals. After centrifugation, the Cr(VI) reduction was followed by measuring the absorbance at 348 nm with UV–visible spectrophotometer (Shimadzu UV 1800) using 1 cm path length quartz cell. The concentration was checked by potentiometric titration with the Mohr salt. The photocatalytic tests for hydrogen production were performed in the same reactor reported in our previous work [24]. Hydrogen has been positively identified by gas chromatography; it was determined by measuring the volume with a gas burette and corrected from the blank test. All the chemicals were of reagent grade quality and the solutions made with distilled water.

3. Results and discussion

3.1. Characterization

The semiconductor is the key element of the PEC device, since it has the dual role of photoreceptor and reservoir of electrons. The X-ray diffraction pattern of $CuAl_2O_4$ (Fig. 1), recorded for 10 s at each 0.02° step over the 2θ interval 15–60°, confirms the formation of the spinel structure with a lattice constant of 0.8086 nm in perfect agreement with the JCPDS card No. 33-0448. $CuAl_2O_4$ is nominally non-stoichiometric and the thermal evolution of the conductivity obeys to an Arrhenius type law with an activation energy E_a of 0.16 eV [19]. The electro kinetic parameters, obtained from the semi logarithmic plot (Fig. 2): an exchange current density of 0.33 mA cm^{-2}, a corrosion potential of +0.15 V and a polarization resistance of 143.76 Ω cm^2 indicate a long lived material. The oxide is stable in acidic medium (H_2SO_4, 0.05 M). Over one month, the amount of dissolved copper in the working solution would have been too small for a reliable determination by atomic absorption. $CuAl_2O_4$ has not yet been assessed photoelectrochemically; it is attractive for PEC characterization and the suitable position of the cationic electronic bands makes it interesting to explore. In any study in which a PEC junction SC/electrolyte is built, it is important to determine the flat band potential. The potential V_{fb} is accurately

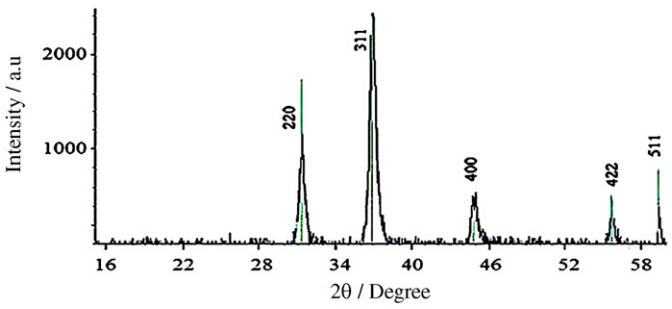

Fig. 1. XRD pattern of the spinel $CuAl_2O_4$ prepared via nitrate way.

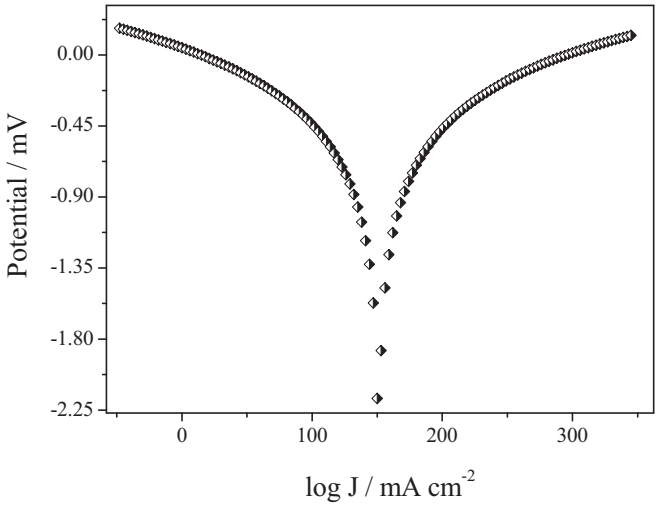

Fig. 2. The cyclic $J(V)$ curve of $CuAl_2O_4$ in acid solution (H_2SO_4, 0.05 M, pH ~2), scan rate 5 mV s^{-1}.

determined from the differential capacitance (Fig. 3):

$$C^{-2} = \left(\frac{2}{Ae\varepsilon\varepsilon_0 N_A}\right)\left(V - V_{fb} - \frac{kT}{e}\right)$$

where all the symbols have their usual meanings. The slope and the intercept to $C^{-2} = 0$ of the Mott Schottky characteristic gave respectively the holes density N_A (4.8×10^{23} m^{-3}) and the potential V_{fb} (0.45 V). The negative slope indicates the p type behavior of $CuAl_2O_4$ and the N_A value characterizes non-degenerate semi conductivity, responsible of a broad depletion layer δ:

$$\delta = \left[\frac{2e\varepsilon\varepsilon_0(V_{fb} - V)}{eN_A}\right]^{0.5}$$

The width δ (76 nm), calculated for a band bending (V_{fb}–V) of 0.5 V, extends over repeat crystallographic units and this is a desirable property in photocatalysis. The permittivity ($\varepsilon \sim 50$) was determined from the dielectric measurements on sintered pellets. $CuAl_2O_4$ exhibits a brown color and both VB and CB are made up of cationic orbital. The photocurrent yield (η) was obtained from dividing the electron flow in the external circuit (from photocurrent

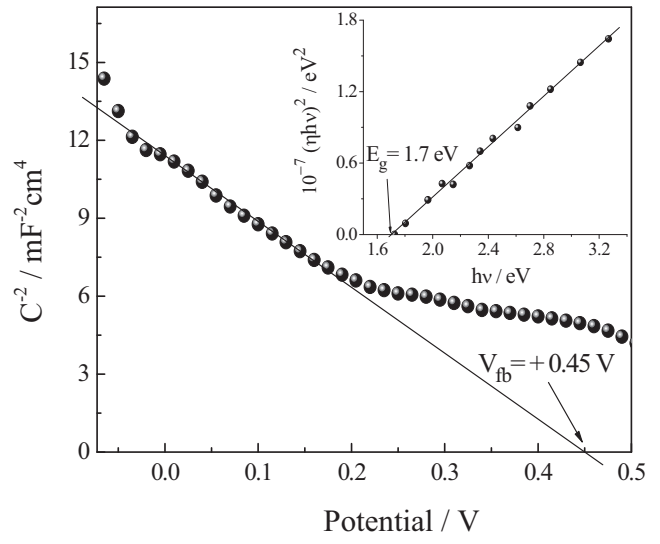

Fig. 3. The Mott–Schottky plot of $CuAl_2O_4$ in H_2SO_4 medium (0.05 M). (Inset) Direct band gap transition of $CuAl_2O_4$.

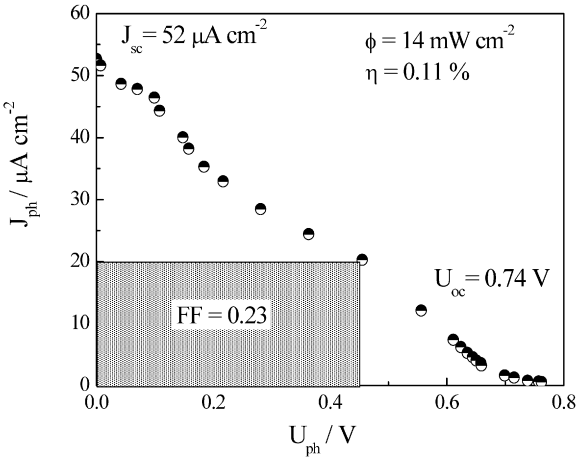

Fig. 4. Photocurrent–photovoltage characteristic of $CuAl_2O_4$ in 0.05 M H_2SO_4 solution under visible light.

J_{ph} subtracted from the dark current) by the incident photon-light measured at each wavelength:

$$\eta = \frac{(J_{ph} - J_d)}{e\phi}$$

ϕ being the flux intensity falling on the electrode and e the elementary charge. The photocurrent–wavelength spectrum has been analyzed to get both the energy and type of interband transitions [25]:

$$(\eta h\nu)^{2/n} = Const(h\nu - E_g)$$

where n equals 1 or 4 respectively for direct or indirect transitions. The electrode was polarized at −0.4 V, a value belonging to the plateau region in the $J_{ph}(V)$ characteristic. Fig. 3(Inset) shows that the plot with n= 1 is linear and the intercept with $h\nu$ axis yields a direct E_g value of 1.70 eV.

3.2. Photocatalysis

The J_{ph}–U_{ph} characteristic of $CuAl_2O_4$ is unsatisfactory although an open circuit potential (U_{oc}) of 0.74 V has been obtained (Fig. 4). The low fill factor (0.23) and the quantum yield (0.11%) are attributed to the high resistive nature of the pellets ($\rho_{300\,K} = 2.6 \times 10^{+3}\ \Omega$ cm). The reason is also due to lack of reversibility of the electrochemical system, i.e. a slow rate of electron transfer of the $HCrO_4^-/Cr^{3+}$ couple on $CuAl_2O_4$. The energy-rich specie Cr^{3+} is formed in a single step causing a large over-potential.

Although it is not a general rule, the photocatalysis is intrinsically governed by the morphology of the material through the active surface. It has been established that the electron flow in low polaron oxides like $CuAl_2O_4$ is the rate determining step. Hence, the crystallite dimension must be comparable with the diffusion length and small size should lead to high quantum efficiency. So, our approach was to elaborate the oxide in nano crystalline morphology of the kind already obtained with the spinels [26]. $CuAl_2O_4$ has been synthesized by nitrate way in order to have a large surface to mass ratio and to decrease the path the electrons have to diffuse before reaching the interface. The PEC characterization allows us to draw the energy band diagram of the hetero-system (Fig. 5) which predicts from a thermodynamical point of view whether the $HCrO_4^-$ reduction and/or hydrogen evolution occurs or not. The crystallite is naturally polarized at the free potential (U_f) and cathodically protected against photo corrosion. So, an additional condition to eventuate in photo reductions is that the potential U_f

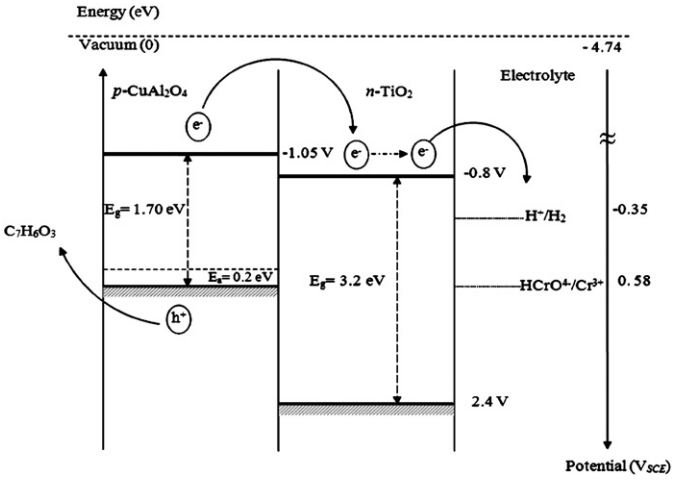

Fig. 5. $CuAl_2O_4/TiO_2$ junction energy diagram.

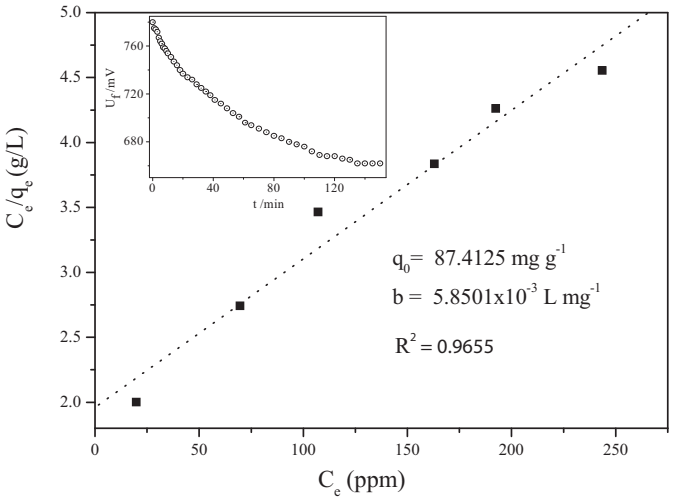

Fig. 6. Langmuir adsorption isotherm plot. C_e: uptake at equilibrium, q_e: adsorption capacity at equilibrium, q_0: maximum adsorption capacity, b: Langmuir's constant. (Inset) Chronopotentiometric profile of Cr(VI) in $CuAl_2O_4$ (25%)/TiO_2 suspension (pH ~2).

(−0.12 V) of p-$CuAl_2O_4$ must be more negative than the potential V_{fb}. It is possible to improve the reliability of the system that affords the catalysis of organics by visible light. As it has already been mentioned in introduction, TiO_2 is chemically stable but absorbs exclusively in the UV region and is of little practical use for the solar energy conversion. The hetero-system is an elegant way to extend the photo response toward longer wavelengths (visible region) and the current matching is determined by the relative position of band gap energy of both SCs. The electronic bands of $CuAl_2O_4$, deriving from cationic parentage, are pH insensitive whereas those of TiO_2 usually vary by 0.06 V pH^{-1}. We have taken advantage of this property and at pH 2, $CuAl_2O_4$-CB is suitably positioned with respect to TiO_2-CB. Equilibrium is established by equalization of the electrochemical potentials of oxides with the transfer of minority carriers (electrons) from the bulk to the interface p-$CuAl_2O_4/n$-TiO_2 resulting in a downward band bending (B). The hetero-system acts in a short circuited configuration through the electrolytic solution and the contact between TiO_2 and $CuAl_2O_4$ particles is ensured mainly by collision. The separation of (e^-/h^+) pairs, generated in the sensitizer $CuAl_2O_4$, occurs through the internal electric field within the depletion layer. The photoelectrons are injected into TiO_2-CB and transferred to $HCrO_4^-$ and/or H_2O species.

The dark adsorption is a precondition to the photocatalysis. The X-ray diffraction reveals the presence of the TiO_2 anatase variety which exhibits an affinity for inorganic ions and a transition period is required before irradiation. The reduction no longer holds if the adsorption is weak and it is tempting to attribute the photoreduction to the strong adsorption (see below). The point of zero charge pzc, the pH at which the net adsorbed surface is zero, was found to be 7.6 and all the experiments were carried out in acidic medium. The adsorption is typically anionic and $HCrO_4^-$ is adsorbed onto the surface catalyst, charged positively. Furthermore, decreasing the pH would move the CB of $CuAl_2O_4$ and TiO_2 toward each other, resulting in enhanced electron transfer. The Langmuir's model is found to be the most adequate in representing the dark adsorption (Fig. 6), the adsorption onto TiO_2 surface is monolayer and reversible, and saturation phenomenon takes place progressively. The maximum adsorption capacity q_0 (87.4 mg/g) and the Langmuir's constant b at 303 K (5.85 L/mg) were determined. The chrono-potentiometry provides a further evidence to support the above point Fig. 6 (inset). The $HCrO_4^-$ solution was equilibrated with the catalyst after ~2 h. The difference between the nominal concentration and that measured after equilibrium was taken as the adsorbed quantity (~55%). The photocatalytic tests were carried out with different Cr(VI) concentrations and the results (Fig. 7a) give an optimal value of 30 ppm. The dependence on the reduced $HCrO_4^-$ at saturation time with various mass ratios $TiO_2/CuAl_2O_4$ is illustrated in Fig. 7b; the photoactivity increases with increasing the ratio up to 3/1 above which it decreases drastically to zero for pure TiO_2. This behavior can be ascribed to the adsorption kinetic, a known phenomenon of heterogeneous catalysis. The extent of the adsorption was enhanced by ~200% when the percentage of TiO_2 was increased from 0% to 25% and by only 11% when further TiO_2 was added (up to 100%). This may be attributed to the increase in the catalyst surface and consequently to the number of active sites dedicated to the pollutant capture which results in improved efficiency of Cr(VI) adsorption. However, the adsorption for the ratio 1/1 remains unclear and subtle, presumably, because of the chemical heterogeneity of the surface. In parallel, the plot exhibited enhanced Cr(VI) photoreduction at higher TiO_2 percentage. Furthermore, the turbidity of the solution and the light scattering also account for the regression of the photoactivity.

One of the major drawbacks limiting the quantum efficiency is the back carriers transfer which results in the recombination process. The potential of $CuAl_2O_4$-VB (0.65 V) lies far below the O_2/H_2O level and water cannot be used as holes scavenger. In order to prevent the accumulation of photoholes, we have used salicylic acid which increases the lifetime of the carriers while maintaining the reducing ability of TiO_2-CB. Oxalic acid has also been tested in a comparison purpose but it has showed less efficiency (Fig. 8a). Salicylic acid is more susceptible to be attacked by strong oxidant such as Cr(VI) due to benzene nucleus. Indeed, the –COOH group results in transfer of nucleophilic π-electron density from the benzene ring to the –COOH group, thus tending to weaken its acidity. On the contrary, oxalic acid is more stable and less likely to be oxidized. In addition, it was reported that the accompanied oxidation of salicylic acid reduces the deactivation effect of the deposited Cr(III) species on the photocatalytic activity of the TiO_2 photocatalyst [12]. Moreover, different works already published showed the synergic effect between the photocatalytic reduction of Cr(IV) and the oxidation of organic compounds [13–15]. The photocatalytic process is confined in a micro reaction space where the bulk phase diffusion of reactants is minimized. Both half electrochemical reactions take place concomitantly and progress with almost equal rates on the opposite poles of the "bifunctional crystallite $CuAl_2O_4/TiO_2$" that behaves like a micro PEC cells. Conceivably, the oxidation of acid occurs on $CuAl_2O_4$ while the chromate reduction proceeds mostly

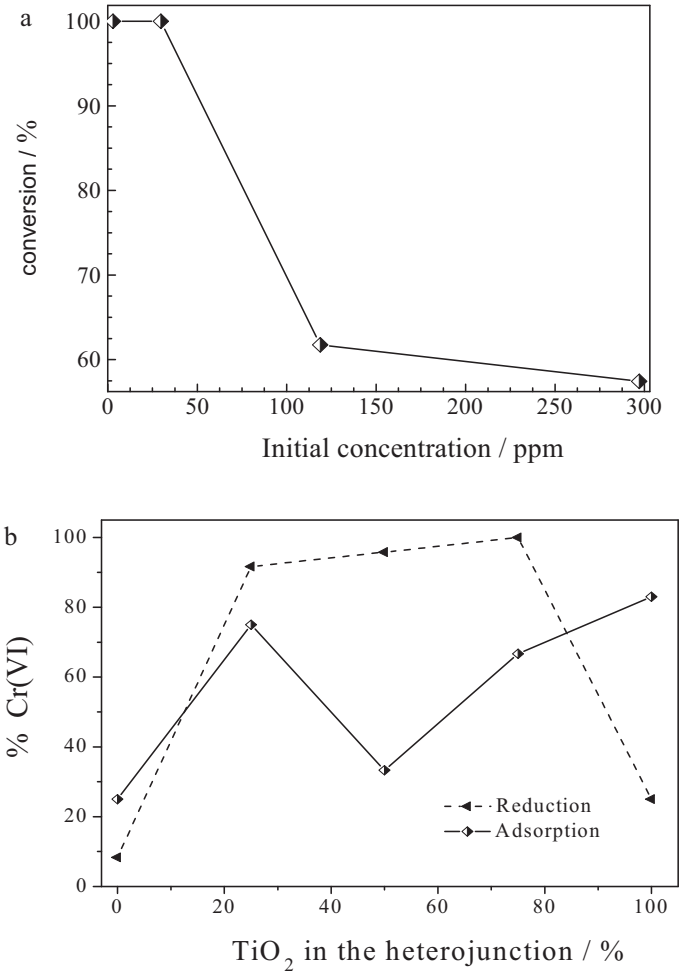

Fig. 7. (a) Effect of initial concentration of Cr(VI) toward the photocatalytic efficiency of $CuAl_2O_4$ (25%)/TiO_2. (b) Photocatalytic reduction of Cr(VI) as function of TiO_2 mass in the hetero-junction with the following experimental conditions: $CuAl_2O_4$ (25% wt.)/TiO_2, Cr(VI) concentration: 30 ppm pH ~2, volume of the solution 200 mL.

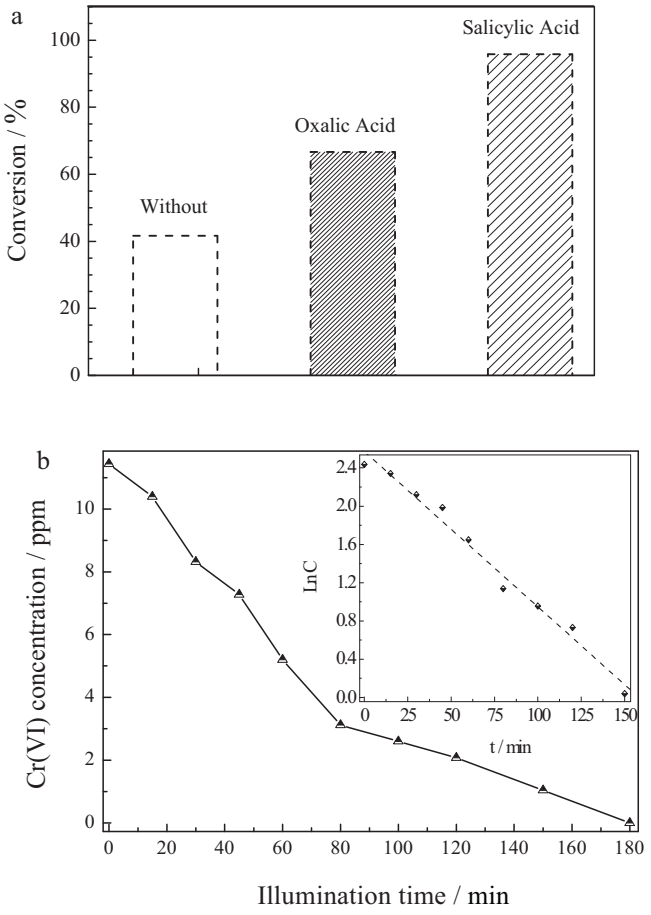

Fig. 8. (a) Cr(VI)% reduction in presence of oxalic acid and salicylic acid in acidic medium. (b) Photocatalytic conversion kinetic of Cr(VI) under the same experimental conditions as in Fig. 7.

on TiO_2. The degradation of salicylic acid under various conditions has already been studied [27] but the details of its conversion have not been clarified yet. The complete mineralization occurs through photo oxidative pathway by both photo holes and dissolved oxygen. The p-$CuAl_2O_4$/n-TiO_2 junction has the thermodynamic force to catalyze the downhill reaction:

$$4HCrO_4^- + 3C_7H_6O_3 + 18O_2 + 16H^+ \rightarrow 4Cr^{3+} + 21CO_2 + 19H_2O$$

with a free enthalpy of $-557\,kcal\,mol^{-1}$ [28]. Since 12 electrons are involved in the reaction, this corresponds to ~2 V/chromium. A transfer of three electrons per $HCrO_4^-$ molecule is required and the quantum efficiency (η) of the light conversion is given by:

$$\eta = 3\{\text{number of converted } HCrO4^- \text{ mol s}^{-1}/\text{photons flux s}^{-1}\}$$

Taking into account both adsorption and photoreduction, the Langmuir–Hinshelwood model of photocatalysis is dedicated to assess the chromium reduction rate. It suggests a reaction occurring between adsorbed species on the surface catalyst whose rate is proportional to adsorption flow. The linear plot of log [$HCrO_4^-$]-time indicates that the reduction obeys to a first order kinetic (Fig. 8b). The apparent reaction constant (k_{app}) averages $1.62 \times 10^{-2}\,min^{-1}$ with a quantum yield of 0.11%. The half life, the time needed for the concentration to fall to half of its initial value, is found to be concentration independent and averages 1 h. Over illumination time, the UV band intensity (348 nm) decreased and a new one appeared at 547 nm due to the generation of Cr^{3+} as compared with standard $Cr(NO_3)_3$ (Fig. 9). The light absorption of $CuAl_2O_4$ interferes with that of $HCrO_4^-$ ions which act as optical filter but reduces only slightly the flux intensity at low concentration (10^{-4} M). Indeed, the absorption of $HCrO_4^-$ is low in the green region of spectrum; at 450 nm 10% adsorption for 1 cm path length is reported.

The Cr(VI) reduction decelerates after less than 1 h of continued irradiation. This tendency to saturation is due to the competitive water reduction. This can be clearly understood with the help of the band diagram by the relation between the energy levels of TiO_2-CB and H_2O/H_2 couple (Fig. 5). The photoelectrons in TiO_2-CB can reduce chromate and/or water and this is important for the solar energy conversion where a particular goal is desired. A great concern has been focused upon hydrogen as clean energy. Currently most production comes from methane reforming processes which spew huge amounts of CO_2 in the atmosphere, responsible of the global warming. For an efficient activity, a positive potential of the conduction band and good absorption properties in the visible region are required, two conditions fulfilled by p-$CuAl_2O_4$. Over TiO_2, the potential of the couple H_2O/H_2 was found to be (−0.35 V) [29]. The hydrogen evolves with an average rate of $3.75\,cm^3\,(g\,catalyst)^{-1}\,h^{-1}$, and decreases over time as the volume approaches a plateau region after 1 h illumination (Fig. 10). Salicylic acid has already been found to promote Cr(VI) reduction and to lower the deactivation effect of the deposited Cr(III) species on TiO_2 catalyst [12]. Therefore, the presence of organic acid would enhance

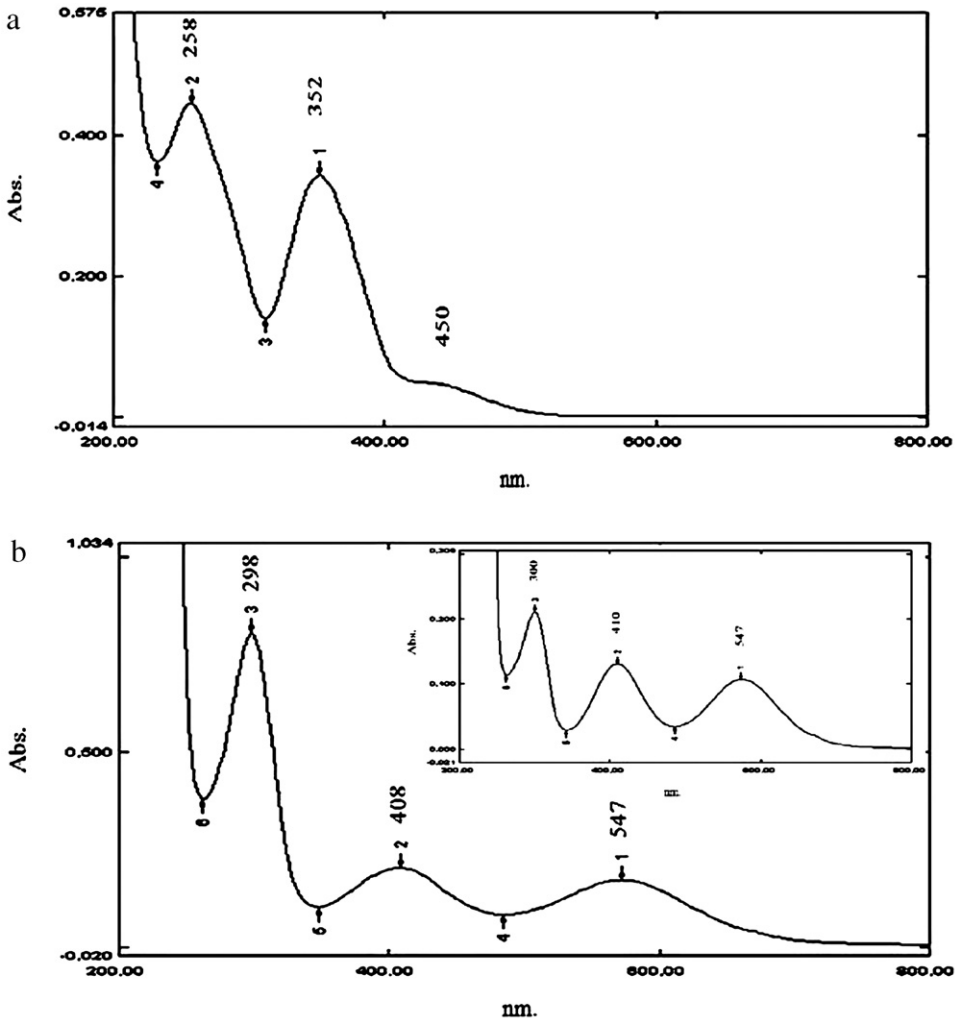

Fig. 9. UV–visible spectra of: (a) Initial solution of Cr(VI), (b) 3 h illuminated solution, (b inset) standard $Cr(NO_3)_3$.

both the Cr(VI) photoreduction and hydrogen evolution. The photocatalytic results are quite encouraging and can be extended to a stirred reactor. These issues are presently under way and will be considered in ongoing issues.

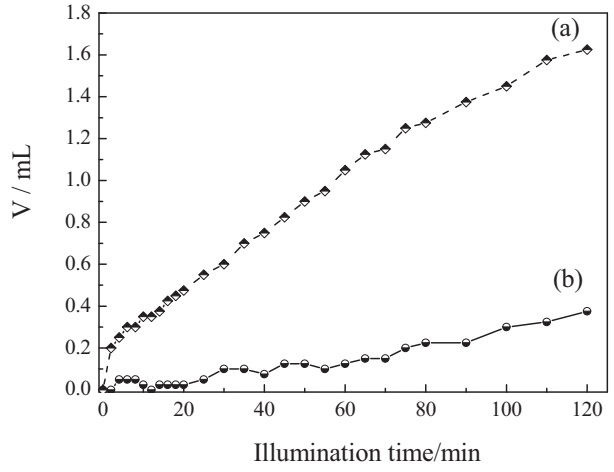

Fig. 10. Volume of evolved hydrogen vs illumination time for p-$CuAl_2O_4$/n-TiO_2. (a) Presence of salicylic acid and Cr(VI), (b) Cr(VI) alone.

4. Conclusion

The ability of the hetero-system $CuAl_2O_4/TiO_2$ for the $HCrO_4^-$ reduction under visible light has been demonstrated. The nitrate route was used for the synthesis of fine photoactive particles. $CuAl_2O_4$ is long lived, and has been assessed photoelectrochemically; the Langmuir model suitably fit the adsorption data. The light doping provides a wide depletion layer with the occurrence of the photo effect thanks to the high energetic position of the conduction band of $CuAl_2O_4$. The reaction involves cheap and available reactants; the mass ration has been optimized and the chromate photoreduction is greatly enhanced in presence of salicylic acid owing to the efficient separation of (e^-/h^+) pairs, and follows a first order kinetic according to Langmuir–Hinshelwood model. The Cr(VI) reduction takes place in competition with the water discharge which seems to be the main reason for the deceleration process, as evidenced by the bending over the curve. Taking these findings into account, we feel that detailed studies with stirred reactor will be required before an efficient photoelectrochemical system is realized.

Acknowledgments

We are very grateful to the Faculty of Chemistry (Algiers) for its financial support. We would like to acknowledge M. Kebir for his

technical assistance, and Mme B. Bouchali for providing linguistic scrutiny.

References

[1] Y. Gong, X. Liu, L. Huang, W. Chen, Stabilization of chromium: an alternative to make safe leathers, J. Hazard. Mater. 179 (2010) 540–544.

[2] M. Gheju, A. Iovi, I. Balcu, Hexavalent chromium reduction with scrap iron in continuous-flow system. Part 1. Effect of feed solution pH, J. Hazard. Mater. 153 (2008) 655–662.

[3] U. Danis, Chromate removal from water using red mud and crossflow microfiltration, Desalination 181 (2005) 135–143.

[4] C. Das, P. Patel, S. De, S. DasGupta, Treatment of tanning effluent using nanofiltration followed by reverse osmosis, Sep. Purif. Technol. 50 (2006) 291–299.

[5] A. Asem, Atia, Synthesis of a quaternary amine anion exchange resin and study its adsorption behaviour for chromate oxyanions, J. Hazard. Mater. B 137 (2006) 1049–1055.

[6] M. Boroski, A.C. Rodrigues, J.C. Garcia, A.P. Gerola, J. Nozaki, N. Hioka, The effect of operational parameters on electrocoagulation–flotation process followed by photocatalysis applied to the decontamination of water effluents from cellulose and paper factories, J. Hazard. Mater. 160 (2008) 135–141.

[7] J.Y. Edward, H. Janet, M. Samantha, W. Su, Photochemical reduction of hexavalent chromium in glycerol-containing solutions, J. Environ. Pollut. 117 (2002) 1–3.

[8] J. Blanco, S. Malato, P. Fernández-Ibáñez, D. Alarcón, W. Gernjak, M.I. Maldonado, Review of feasible solar energy applications to water processes, Renew. Sustain. Energy Rev. 13 (2009) 1437–1445.

[9] N. Wang, L. Zhu, K. Deng, Y. She, Y. Yu, H. Tang, Visible light photocatalytic reduction of Cr(VI) on TiO_2 in situ modified with small molecular weight organic acids, Appl. Catal. B Environ. 95 (2010) 400–407.

[10] L. Yang, Y. Xiao, S. Liu, Y. Li, Q. Cai, Sh. Luo, Guangming Zeng, Photocatalytic reduction of Cr(VI) on WO_3 doped long TiO_2 nanotube arrays in the presence of citric acid, Appl. Catal. B Environ. 94 (2010) 142–149.

[11] J. Sun, J.-D. Mao, H. Gong, Y. Lan, Fe(III) photocatalytic reduction of Cr(VI) by low-molecular-weight organic acids with α-OH, J. Hazard. Mater. 168 (2009) 1569–1574.

[12] N. Wang, Y. Xu, L. Zhu, X. Shen, H. Tang, Reconsideration to the deactivation of TiO_2 catalyst during simultaneous photocatalytic reduction of Cr(VI) and oxidation of salicylic acid, J. Photochem. Photobiol. A: Chem. 201 (2009) 121–127.

[13] L. Wang, N. Wang, L. Zhu, H. Yu, H. Tang, Photocatalytic reduction of Cr(VI) over different TiO_2 photocatalysts and the effects of dissolved organic species, J. Hazard. Mater. 152 (2008) 93–99.

[14] B. Xie, H. Zhang, P. Cai, R. Qiu, Y. Xiong, Simultaneous photocatalytic reduction of Cr(VI) and oxidation of phenol over monoclinic $BiVO_4$ under visible light irradiation, Chemosphere 63 (2006) 956–963.

[15] S. Chakrabarti, B. Chaudhuri, S. Bhattacharjee, A.K. Ray, B.K. Dutta, Photoreduction of hexavalent chromium in aqueous solution in the presence of zinc oxide as semiconductor catalyst, Chem. Eng. J. 153 (2009) 86–93.

[16] T. Aarthi, G. Madras, Photocatalytic reduction of metals in presence of combustion synthesized nano-TiO_2, Catal. Commun. 9 (2008) 630–634.

[17] J. Claverie, G. Campet, D. Conte, G. Le Flem, H.P. Egenmuller, Influence of covalent bonding on the photoelectrochemical properties of some Perovskite-type related compounds, J. Phys. Status Solidi A 77 (1983) 603.

[18] A. Boudjemaa, R. Bouarab, S. Saadi, A. Bouguelia, M. Trari, Photoelectrochemical H_2-generation over Spinel $FeCr_2O_4$ in X^{2-} solutions (X^{2-} = S^{2-} and $SO^{2-}{}_3$), J. Appl. Energy 86 (2009) 1080–1086.

[19] S. Saadi, A. Bouguelia, M. Trari, Photoassisted hydrogen evolution over spinel CuM_2O_4 (M = Al, Cr, Mn, Fe and Co), J. Renew. Energy 31 (2006) 2245–2256.

[20] S. Bassaid, M. Chaib, S. Omeiri, A. Bouguelia, M. Trari, Photocatalytic reduction of cadmium over $CuFeO_2$ synthesized by sol–gel, J. Photochem. Photobiol. A: Chem. 201 (2009) 62–68.

[21] J. Yan, L. Zhang, H. Yang, Y. Tang, Z. Lu, S. Guo, Y. Dai, Y. Han, M. Yao, $CuCr_2O_4/TiO_2$ heterojunction for photocatalytic H_2 evolution under simulated sunlight Irradiation, J. Sol. Energy 83 (2009) 1534–1539.

[22] R. Brahimi, Y. Bessekhouad, A. Bouguelia, M. Trari, $CuAlO_2/TiO_2$ heterojunction applied to visible light H2 production, J. Photochem. Photobiol. A: Chem. 186 (2007) 242–247.

[23] Y. Bessekhouad, D. Robert, J.V. Weber, Preparation of TiO_2 nanoparticles by sol–gel route, J. Photoenergy 5 (2003) 153–158.

[24] S. Saadi, A. Bouguelia, A. Derbal, M. Trari, Hydrogen photoproduction over new catalyst $CuLaO_2$, J. Photochem. Photobiol. A: Chem. 187 (2007) 97–104.

[25] J.I. Pankov, Optical Processes in Semiconductors, Dover, New York, 1971.

[26] S. Boumaza, A. Bouguelia, R. Bouarab, M. Trari, Physical and photoelectrochemical studies for hydrogen photo-evolution over the spinel $ZnCr_2O_4$, Int. J. Hydrogen Energy 34 (2009) 4963–4967.

[27] G. Colón, M.C. Hidalgo, J.A. Navío, Photocatalytic deactivation of commercial TiO_2 samples during simultaneous photoreduction of Cr(VI) and photooxidation of salicylic acid, J. Photochem. Photobiol. A: Chem. 138 (2001) 79–85.

[28] D.R. Stull, E.F. Westrum Jr., G.C. Sinke, The Chemical Thermodynamics of Organic Compounds, John Wiley and Sons, New York, 1969.

[29] M. Kaneko, I. Okura, Photocatalysis Science and Technology, Springer, Kodansha, 2002.